**Article:**
Tessin, A orcid.org/0000-0001-8657-8484, Bianchi, TS, Sheldon, ND et al. (3 more authors) (2017) Organic matter source and thermal maturity within the Late Cretaceous Niobrara Formation, U.S. Western Interior. Marine and Petroleum Geology, 86. pp. 812-822. ISSN 0264-8172

https://doi.org/10.1016/j.marpetgeo.2017.06.041

# Organic Matter Source and Thermal Maturity within the Late Cretaceous Niobrara Formation, U.S. Western Interior

Allyson Tessin[1,2,*], Thomas S. Bianchi[3], Nathan D. Sheldon[1], Ingrid Hendy[1], Jack A. Hutchings[3], T. Elliott Arnold[3]

[1]Department of Earth and Environmental Sciences, University of Michigan, Ann Arbor, MI 48109
[2]School of Earth and Environment, University of Leeds, Leeds LS2 9JT, UK
[3]Department of Geological Sciences, University of Florida, Gainesville, FL 32611
*Corresponding author: a.c.tessin@leeds.ac.uk

## Abstract

The Late Cretaceous sedimentary record of the North American Western Interior Seaway is characterized by cyclic deposition of organic carbon-rich sediments. One notable interval during the late Coniacian-Santonian is recorded by the Niobrara Formation. The organic carbon-rich interval within the Niobrara Formation has been identified as Oceanic Anoxic Event (OAE) 3. Understanding the reason for this distribution of organic carbon within the Niobrara Formation requires a refined understanding of the source and maturity of the organic matter. In this study, we present lipid biomarker records from the USGS Portland #1 core (Cañon City, CO) to constrain the thermal maturity of the organic matter and the differing contributions of organic matter sources. Sterane and hopane thermal maturity indices indicate that the samples are somewhat immature with respect to oil formation and that there is strong agreement between different proxies for thermal maturity. Based on the distribution of n-alkanes, steranes, and hopanes, there is a significant increase in the contribution of algal organic matter during and after OAE 3, coeval with increased organic carbon accumulation. Although a consistent terrestrial contribution is observed, it is only a minor source of organic matter at the Portland core location and does not drive increased organic matter accumulation during OAE 3. Of particular note is the consistent influence of even-over-odd predominantly mid-chain length ($C_{21}$ to $C_{25}$) organic matter. This observation

within the brackish to marine, not methanogenic WIS represents an expansion of the depositional settings in which even-over-odd predominance has been observed in mid-chain length n-alkanes. Pristane (Pr) and phytane (Ph) abundances are inconsistent with a redox control on Pr/Ph ratios and suggest an increase in the delivery and/or preservation of phototrophic organic matter as the source for pristane and phytane in the Portland core.

Keywords: Organic carbon; lipid biomarkers; Oceanic Anoxic Events; Western Interior Seaway

## 1.0 Introduction

Late Cretaceous deposition in the North America Western Interior Seaway (WIS) is characterized by cyclic deposition of organic carbon-rich sediments (e.g. Pratt et al., 1993; Dean and Arthur, 1998; Meyers et al., 2005), particularly during Oceanic Anoxic Events (OAEs) 2 and 3 (Meyers et al., 2005; Locklair et al., 2011). The Niobrara Formation in the WIS records the latter event, which is of particular interest because, although it is not a global event (Wagreich, 2012), it represents a prolonged period (~3 Ma) of elevated sedimentary organic carbon accumulation within the WIS (Locklair et al., 2011; Tessin et al., 2015). The organic carbon-rich deposits from the Niobrara Formation continue to be of interest within the petroleum industry as a self-sourced resource play, especially with the advent of new technologies for oil shale extraction (Sonnenberg, 2011).

Sedimentary sequences that include the transition from low organic carbon accumulation to black shale deposition provide an opportunity to determine the causes of enhanced organic carbon accumulation. Sediments deposited within the Niobrara Formation include this transition from organic carbon-poor (0–2%) to organic carbon-rich (up to 10%). The Niobrara Formation is formally sub-divided into two members: the Fort Hays Limestone and the Smoky Hill Chalk. The basal Fort Hays Limestone is relatively organic-carbon poor

and consists of ledge-forming limestone beds separated by thin shales (Scott and Cobban, 1964). The overlying Smoky Hill Chalk was sub-divided by Scott and Cobban (1964) into seven informal units (the lower shale limestone (LSL), the lower shale (LS), the lower limestone (LL), the middle shale (MS), the middle chalk (MC), the upper shale (US), and the upper chalk (UC)). Previous research has identified OAE 3 in the LS and LL units of the Smoky Hill Chalk based on a positive $\delta^{13}C$ excursion and elevated organic carbon concentrations (e.g. Locklair et al., 2011; Tessin et al., 2015). The basal LSL unit of the Smoky Hill Chalk was deposited under conditions similar to the Fort Hays Limestone (Tessin et al., 2015), therefore, for our purposes, the Fort Hays Limestone and the LSL unit will be referred to as Interval 1. Interval 2 is defined by the positive $\delta^{13}C$ excursion and includes the LS and LL units of the Smoky Hill Chalk. Interval 3 includes the MS unit of the Smoky Hill Chalk. Intervals 1 and 2 are characterized by variable but high carbonate concentrations (average ~70%). The transition between the LL and MS units (Intervals 2 and 3) is marked by a decrease in carbonate concentrations (average ~40%; Locklair et al. 2011; Tessin et al., 2015).

Organic carbon accumulation was low (<2%) during Interval 1 and biological and geochemical proxy evidence suggests that the WIS was dominantly oxic during this time (Savrda, 1998; Tessin et al., 2015; Tessin et al., 2016; Lowery et al., 2017). Organic matter preserved within Interval 1 is characterized by low organic carbon to nitrogen ratios (C:N) and low hydrogen index values (Tessin et al., 2015). This nitrogen-rich and hydrogen poor organic matter has been interpreted as either predominantly terrestrial in origin or oxidized marine organic matter (Tessin et al., 2015). During Intervals 2 and 3, deposition occurred under oxygen limited conditions (Savrda, 1998; Tessin et al., 2015; Tessin et al., 2016; Lowery et al., 2017). At the onset of Interval 2 the elemental and isotopic composition of sedimentary organic matter changes (Tessin et al., 2015). Organic matter deposited within

Intervals 2 and 3 is more nitrogen-poor and hydrogen-rich than Interval 1, indicating a change in the preservation and/or source of organic matter (Tessin et al., 2015).

Despite significant research on the Niobrara Formation, the fundamental question of how the source of organic matter changes throughout the formation remains unanswered. In this study, we present lipid biomarker records from the USGS Portland core to evaluate the thermal maturity and variations in organic matter source within the Niobrara Formation to characterize the organic matter accumulated before, during, and after the previously identified "OAE 3" interval. The degree of thermal maturity is evaluated first, because increasing maturity can significantly alter biomarker distributions and complicate paleoenvironmental reconstructions. Organic thermal maturity is assessed, using sterane and hopane stereochemistry indices (Mackenzie et al., 1980; Seifert and Moldowan, 1986), and compared with previous RockEval and vitrinite reflectance-derived estimates of thermal maturity (Locklair, 2007). The evolving sources of organic matter within the WIS are subsequently evaluated using the distribution of n-alkanes, steranes $C_{27}$–$C_{30}$ and sterane/hopane ratios in order to distinguish between organic matter sources including marine phytoplankton and zooplankton, higher plants, algae, and bacteria (e.g. Moldowan et al., 1985; Peters et al., 2005). Finally, the pristane and phytane ratios are compared with previous biological and geochemical estimates of paleo-redox conditions to evaluate the viability of this proxy for reconstructing redox conditions in the geologic past.

## 2.0 Methods and materials

The USGS #1 Portland core was drilled and continuously cored near Cañon City, CO (Dean and Arthur, 1998). The Portland core is located within the deep, central axis of the WIS; this region contains a complete record of the onset of black shale deposition (Figure 1). It is also located outside of the most thermally-mature regions of the basin, where more

thermal alteration of organic matter might be expected. Significant work has been conducted on the Portland core, which allows for comparison to other biological and geochemical studies (Savrda, 1998; Locklair et al. 2011; Tessin et al., 2015; Tessin et al., 2016; Lowery et al., 2017). The 75-m thick Late Cretaceous Niobrara Formation section of the Portland core was sampled at 0.5 m resolution at the USGS Core Research Center in Denver, CO (Figure 1). Chemostratigraphy for the core is based on carbon isotope and total organic carbon (TOC) records presented in Tessin et al. (2015), which were used to identify Intervals 1, 2, and 3.

Samples analyzed for organic geochemical analyses were ground to <75 μm and homogenized in an alumina shatterbox. Between 5 and 20 g of sample was then extracted on a Dionex Automated Solvent Extractor (ASE) 300 with a 9:1 dichloromethane:methanol (DCM:MeOH) mixture at 100°C and 1500 psi. Each extract was evaporated to dryness under a gentle stream of $N_2$. The apolar fraction was separated using silica open column chromatography by elution with 3 mL hexane. The eluent was then dried under a gentle stream of $N_2$ and stored at 4°C before final analysis.

Apolar compounds were identified via gas chromatography-mass spectrometry (ThermoScientific Q8000 Triple Quadropole MS paired to a Trace 1310 Gas Chromatograph) and compared with retention times of reference compounds. Mass spectrometer data was analyzed using OpenChrom. The abundances of steranes and hopanes were determined based on masses of m/z 217 and 191, respectively. Odd/even preferences of long-chain length n-alkanes were determined using carbon preference index (CPI) and odd-even predominance centered at n-$C_{31}$ ($OEP_{31}$), which were calculated as follows:

$$CPI = \frac{2(n-C_{23}+n-C_{25}+n-C_{27}+n-C_{29})}{n-C_{22}+2(n-C_{24}+n-C_{26}+n-C_{28})+n-C_{30}} \quad \text{(Bray and Evans, 1961)} \qquad (1)$$

$$OEP_{31} = \frac{n-C_{29}+6(n-C_{31})+n-C_{33}}{4(n-C_{30}+n-C_{32})} \quad \text{(Scanlon and Smith, 1970)} \qquad (2)$$

Mid-chain length odd-even predominance was calculated based on by adapting $OEP_{31}$ and calculating the OEP of n-alkanes 21–25. The terrigenous/aquatic ratio (TAR) was used to evaluate the relative abundance of long-chain ($C_{27}$–$C_{31}$) to short-chain ($C_{15}$–$C_{19}$) n-alkanes as follows:

$$TAR = \frac{n-C_{27}+n-C_{29}+n-C_{31}}{n-C_{15}+n-C_{17}+n-C_{19}} \quad \text{(Bourbonniere and Meyers, 1995)} \qquad (3)$$

## 3.0 Results and discussion

### 3.1 Sterane and hopane thermal maturity indices

Thermal maturity is generally defined as the extent of alteration of organic matter by heat-driven reactions — an important process in the conversion of sedimentary organic matter to petroleum. A series of biomarker indices used to evaluate the degree of thermal maturity (Figure 3) have been developed based on the predictable transformation of the stereochemical configuration of terpanes and steranes - associated with increasing thermal maturity (see Peters et al. (2005) for discussion of biomarker stereochemistry). For example, as thermal maturity increases, the isomerization of C-20 in the $C_{27}$ and $C_{29}$ 5α,14α,17α(H)-steranes has been shown to increase the 20S/(20S+20R) from 0 to an equilibrium value of 0.55 (Seifert and Moldowan, 1986). Similarly, the isomerization of 17α-hopanes at C-22 from S to R is predictable, with values of 22S/(22S+22R) increasing from 0 to 0.6 with maturation (Seifert and Moldowan, 1986). Moretane/hopane ratios provide an additional constraint of thermal maturity, because the βα configuration (moretanes) is thermally less stable than the αβ configuration (hopanes). Abundances of $C_{30}$ moretanes typically decrease relative to $C_{30}$ hopanes with increasing thermal maturity from ~0.8 to 0.05, with most oils

from pre-Cenozoic source rocks showing moretane/hopane ratios of <0.1 (Mackenzie et al., 1980; Seifert and Moldowan, 1986; Peters et al., 2005).

Representative m/z 217 and 191 chromatograms from the lower (62.8 m) and upper (30.4) portions of the core show the abundances of steranes and terpanes (Figure 2). The 20S/(20S+20R) ratios for the $C_{27}$ and $C_{29}$ steranes range from 0.13−0.34 and 0.21−0.31, respectively (Table 1; Figure 3). These sterane 20S/(20S+20R) values indicate that the samples analyzed are thermally immature (Figure 3a). Low hopane abundances in Interval 1 precluded calculation of hopane-based indices (Table 1; Figure 2). The $C_{31}$ hopane 22S/(22S+22R) ratio varies between 0.54−0.59, while the $C_{30}$ hopane to moretane ratio ranges from 0.11−0.21 (Table 1; Figure 3b). The $C_{31}$ hopane 22S/(22S+22R) and $C_{30}$ moretane/hopane ratios are close to equilibrium values (Seifert and Moldowan, 1986; Peters et al., 2005), which indicate maturity close to early oil production (Figure 3). These results, suggestive of organic matter that is nearing early oil formation, further support previous thermal maturity estimates derived from vitrinite reflectance and maximum temperature ($T_{max}$; Locklair, 2007; Figures 3c and 3d; Supplemental Table 1). Consistency between biomarker and other thermal maturity indicators suggests that thermal maturity should not be an issue when interpreting results.

### 3.2 Distribution of n-alkanes

If the distribution of organic carbon is associated with changing organic matter sources in the Portland core, it is critical to know something about the sources of organic matter. The distribution of n-alkanes can be used to assess the relative contribution of algal and terrigenous organic matter, because short-chain n-alkanes (n-$C_{15}$ to n-$C_{19}$) are predominantly derived from marine algae (Collister et al., 1992), whereas long-chain n-alkanes (>n-$C_{25}$) are derived from higher plant waxes (Peters et al., 2005).

Characteristic m/z 57 chromatograms from the lower (62.8 m) and upper (30.4) portions of the core show the relative abundances of n-alkanes (Figure 4). The n-alkane distribution in the Portland core samples is dominated by mid-chain n-alkanes that are reflective of intermediate sources of algal and terrestrial end members (Figures 4 and 5; Supplemental Table 2). In general, all samples include a major proportion of mid-chain length n-alkanes ($C_{21}$–$C_{25}$), whereas long-chain n-alkanes (>$C_{25}$) comprise only a small fraction of all samples. In samples between 70.16 and 59.79 m, short-chain length n-alkane (<$C_{20}$) abundance is relatively low compared to mid-chain length n-alkanes (Figure 5).

Organic matter with a biomarker composition predominantly characterized by odd molecular weight, mid-chain length n-alkanes is typically derived from macrophytes (Viso et al., 1993; Ficken et al., 2000). However, within the $C_{21}$ to $C_{25}$ n-alkanes, odd-over-even predominance is not consistently observed. In fact, the calculated odd-even-preference for mid-chain n-alkanes ($C_{21}$ to $C_{25}$) indicates an even-over-odd predominance in all samples, except at 9.65 and 59.79 m (Table 2). Furthermore, in seven of the fifteen Portland core samples (25.27, 30.38, 34.93, 40.01, 45.09, 62.84, and 68.86) n-$C_{22}$ is the most abundant n-alkane, compared to four samples (15.14, 20.19, 59.79, and 70.16), in which n-$C_{21}$ is the most abundant n-alkane (Figure 5), indicating that macrophytes are not likely the only source of the mid-chain length n-alkanes preserved in these samples. Organic matter characterized by the dominance of n-$C_{22}$ alkanes has been observed in many pre-Miocene source rocks; however, the primary source of the n-$C_{22}$-dominated organic matter remains enigmatic (Schenck, 1968) - an enigma that extends to our results.

Even-over-odd predominance within n-$C_{12}$ to n-$C_{22}$, although atypical, has been observed in a number of recent sedimentary systems and is linked to contributions from algae, bacteria, fungi, and yeast (Nishimura and Baker, 1986; Grimalt and Albaiges, 1987). However, n-$C_{17}$ is consistently the most dominant short-chain length n-alkane in the Portland

core, indicating that the even-over-odd predominance found in the mid-chain length, is not found in short-chain alkanes. Even-over-odd predominance in $C_{22}$ to $C_{30}$ has also been observed in sedimentary records (Welte and Waples 1973; Tissot et al. 1977; Ogihara and Ishiwatari 1998), but was attributed to hypersaline or hydrothermal environments, of which the Coniacian-Santonian WIS was neither. More recently, an even-over-odd predominance was reconstructed within OAE 1 deposits in the Basque-Cantabrian Basin, which was neither hypersaline nor hydrothermal (Chaler et al., 2005). In this case, the even-over-odd predominance was attributed to highly reducing conditions and the presence of methanogenic bacteria (Chaler et al., 2005). However, the even-over-odd predominance in the Portland core is associated with both oxidizing and reducing sedimentary conditions and an absence of biomarkers for methanogenic bacteria, suggesting that redox conditions are not driving the enigmatic n-alkane distribution. The Portland core was deposited under neither hypersaline nor hydrothermal conditions and exhibits no evidence for the presence of methanogenic bacteria. Therefore, even-over-odd predominance within $C_{21}$ to $C_{25}$ likely reflects different organic matter sources than from previous studies (e.g., Welte and Waples 1973; Tissot et al. 1977; Ogihara and Ishiwatari 1998; Chaler et al., 2005).

A shift occurs in the n-alkane records at the onset of Interval 2 (OAE 3), which marks the onset of increased organic carbon accumulation. Compared to underlying samples, especially 59.79 and 62.84, the contribution of short-chain length (algal) n-alkanes increases and remains significant throughout Intervals 2 and 3 (Figures 4 and 5). The increase in organic matter with algal chain-length characteristics at the onset of Interval 2 likely represents an increase in algal productivity and/or increased preservation of “labile” organic matter – characterized by short-chain length n-alkanes.

In addition to short and mid-chain length n-alkanes, all Portland core samples contain long-chain n-alkanes, indicating some contribution from terrestrial-derived organic matter.

The contribution of long-chain n-alkanes is relatively small and invariable, suggesting that changes in terrestrial input are unlikely driving changes in the distribution of organic carbon throughout the Niobrara Formation. The presence of terrestrial plant-derived organic matter is typically verified based on the presence of predominantly odd molecular weight n-alkanes, between $C_{25}$ and $C_{35}$, which are linked with inputs of wax lipids derived from higher plants (Eglinton and Hamilton, 1967; Hedberg, 1968; Peters et al., 2005). Throughout the record, the carbon preference index (CPI) values range from 0.94 to 1.12 (Table 2). However, determination of odd-or-even predominance in our samples is complicated by low abundances of n-alkanes >$C_{33}$. Furthermore, in some samples mid-chain length n-alkanes exhibit an even-over-odd predominance while longer chain n-alkanes in the same sample show an odd-over-even predominance. With these factors in mind, we favor the $OEP_{31}$ index (Scanlon and Smith, 1970), which is based only on n-alkanes between n-$C_{29}$ and n-$C_{33}$. Odd-even-preference ($OEP_{31}$) values vary between 1.22 and 1.75, with the lowest values recorded between 34.93−45.01 m and 59.79−68.86 m (Table 2). The $OEP_{31}$ results indicate a consistent odd-over-even preference in the long-chain alkanes, supporting a terrestrial source for the long-chain n-alkanes (Table 3). Conversely, the CPI, which integrates results from n-$C_{22}$ to n-$C_{30}$, does not show a significant odd-over-even predominance, likely due to the high abundance of n-$C_{22}$ and n-$C_{24}$ in some samples. The Terrestrial-Aquatic Ratios (TAR) offers an additional way to assess the relative contributions of terrigenous (e.g. terrestrial plant) and aquatic (e.g. aquatic algae) organic matter, by comparing the abundances of short- and long-chain length n-alkanes (Meyers, 1997). TAR values in Portland core samples range between 0.23 to 1.84, with all but two samples (at 59.79 and 62.84 m; Figure 6, Table 2) indicating a dominantly aquatic organic matter source (TAR <1), . It must be noted, however, that TAR values can potentially overestimate terrigenous influence because of preferential preservation of more refractory, terrestrially-derived organic matter (Volkman et al., 1987).

### 3.3 Sterane and hopane distribution

The distribution of $C_{27}$–$C_{29}$ steranes can be used to differentiate sources of organic matter further. For example, $C_{27}$ steranes are derived from red algae and zooplankton, and $C_{28}$ steranes are dominant in phytoplankton (green algae and diatoms), with some presence in yeast, fungi, and bacterial plankton, and $C_{29}$ steranes are mostly derived from land plants (Huang and Meinschein, 1979; Volkman, 2003; Peters et al., 2005). Of $C_{27}$ to $C_{30}$ regular steranes, 30–57% are $C_{27}$, 6–32% are $C_{28}$, 27–39% are $C_{29,}$ 2–9% are $C_{30}$ (Figure 6; Table 2). $C_{27}$ is the most abundant sterane in the record, with the exception of samples collected at 40.0 and 45.1 m. A relative increase in $C_{28}$ steranes can be used to evaluate relative algal contributions (Peters et al., 2005). Ratios of steranes $C_{28}$/ ($C_{27}$-$C_{30}$) increase markedly at the onset of Interval 2 and remain elevated throughout the rest of the record (Figure 6), indicating that the contribution of phytoplankton relative to terrestrial plants was greater during Intervals 2 and 3. Further analysis of the relative abundance of these steranes reveals the presence of two distinct pools of organic matter (Figure 7). All samples have a relatively constant (34–40%) contribution of sterane $C_{29;}$ however, low TOC (<1%) samples are characterized by more $C_{27}$, while high TOC (>1%) samples are characterized more by $C_{28}$. As both $C_{27}$ and $C_{28}$ are predominantly sourced from marine organic matter, this suggests a change in either marine source material or preservation. A significant marine algal contribution is further supported by the presence of $C_{30}$ steranes, which are diagnostic of marine chrysophytes, which are known to occur in Cretaceous calcareous and siliceous sediments (Moldowan et al., 1985; Moldowan et al., 1990; Peters et al., 2005). Moreover, the ratio of $C_{30}$/ ($C_{27}$-$C_{30}$) increases up-core (Figure 3), further supporting an increase in the accumulation of algal versus other sources of organic matter during Intervals 2 and 3.

The ratio of steranes/hopanes reflects the relative contribution of eukaryotic (algae and higher plants) vs. prokaryotic (bacteria) organic matter, with higher values indicating a

relative increase eukaryotic organic matter (Moldowan et al., 1985). Sterane/hopane ratios (Figure 6) within the Portland core average 0.04 in samples between 59.8 to 74.2 m before beginning to increase at 55.2 m. Sterane/hopane ratios reach a maximum value of 0.48 at 34.9 m, before subsequently decreasing up-core to a value of 0.22 at 9.7 m. Lower sterane/hopane ratios recorded in the TOC-poor Interval 1, as compared to Intervals 2 and 3, suggest that the relative contribution of eukaryotic organic matter increases coeval with TOC (Figure 6). The overall distribution of alkanes, steranes, and hopanes indicates that at the onset of Interval 2, the contribution of marine algal organic matter to sediments increases abruptly and remains elevated throughout.

### 3.4 Causes of variable organic carbon accumulation within the Niobrara Formation

The shift in n-alkane, sterane, and hopane composition at the transition between Intervals 1 and 2 is marked by an increase in organic carbon accumulation but, is relatively independent of lithologic changes. A lithologic change is marked by the boundary between the Fort Hays Limestone and Smoky Hill Chalk but this occurs ~15 m below the Interval 1 and 2 boundary. The most abrupt lithological change within the Portland record occurs at the transition between Intervals 2 and 3 and is marked by a decrease in carbonate abundance. Alkane, sterane, and hopane abundances do not change dramatically across this boundary, suggesting that these changes are relatively independent of lithology.

The increase in algal organic matter, as shown by changing alkane and sterane distributions, is tightly coupled to increasing TOC values (Figure 7). Therefore, it is likely that all samples contain a relatively minor baseline amount of terrestrial organic matter, and that increased organic carbon accumulation is primarily associated with the enhanced abundance of algal organic matter. It remains difficult to discern whether the increase in algal organic matter at the onset of Interval 2 was driven by enhanced preservation, increased

marine algal productivity, or both. The onset of Interval 2 is characterized by a sea-level high-stand, and is accompanied by changes in major element and trace-metals that reflect deposition under low oxygen conditions (Tessin et al., 2015; Tessin et al., 2016). Coeval changes in the elemental and isotopic composition of organic matter (Tessin et al., 2015) support an increase in the preservation of lipid organic matter under more reducing conditions within Intervals 2 and 3. However, an increase in marine planktonic productivity fueled by the influx of nutrient-rich Tethyan water may have also contributed to the elevated organic carbon burial during this time.

### 3.5 Pristane and Phytane ratios as paleoredox indicators

Most sedimentary pristane and phytane is assumed to derive from the phytyl side-chain of chlorophyll a within phototrophic organisms (e.g. Brooks et al., 1969; Powell and McKirdy, 1973). Sedimentary redox conditions may affect the relative production of the two alkanes during biodegradation of chlorophyll a. Low pristane/phytane ratios (<1) have been interpreted to accompany anoxic sedimentary conditions, as preferential phytane production during reduction of phytol is expected under reducing conditions (Didyk et al., 1978).

The abundances of both pristane and phytane are lowest during Interval 1, particularly between 59.79 and 62.84 m. Pristane and phytane relative abundances increase at the onset of Interval 2 and again at the Interval 2/3 transition. Throughout Interval 3, pristane is the most abundance compound. Pristane to phytane ratios (Pr/Ph) range from 0.98−3.41 (Figure 8). Between 74.2 and 62.8 m, Pr/Ph values average 1.20 (with the exception of an elevated value of 3.40 at 68.9 m) before beginning to increase at 59.8 m. Pr/Ph values then increase to 3.01 at 50.1 m, before falling to 1.25 at 34.9 m. Above 34 m, Pr/Ph abruptly rise and stabilize at an average value of 2.74. Pristane and phytane abundances increase coeval with the increase in short-chain n-alkanes, suggesting that the isoprenoids have an algal source (Figure

5). Of particular note are the elevated pristane abundances within Interval 3 samples coeval with a lithologic shift towards lower carbonate concentrations. If pristane is delivered to the sediments with marine algal organic matter, this correspondence may represent a shift in the planktonic community under lower carbonate preservation and/or production.

The general trend within the Portland core record is lower Pr/Ph values within Interval 1 and elevated Pr/Ph ratios in Intervals 2 and 3. Based on the usual interpretation of Pr/Ph ratios, this would indicate anoxic conditions within Interval 1 and oxic conditions within Intervals 2 and 3. However, when Pr/Ph ratios are compared to inorganic geochemical redox proxies including trace metal concentrations this interpretation is not supported (Figure 8). Molybdenum, for example, is enriched under reducing conditions (e.g. Erickson and Helz, 2000; Chappaz et al., 2014). Molybdenum concentrations from the Portland core indicate that Interval 1 was relatively oxic followed by more reducing conditions during Intervals 2 and 3, demonstrating that the expected relationship between redox conditions and Pr/Ph ratios within the Portland record does not exist (Figure 8). Specifically, the only samples exhibiting Pr/Ph ratios of <1 also have low Mo concentrations, which instead suggests enhanced phytance abundances under relatively oxic sedimentary conditions. Because the Mo concentrations are consistent with other redox sensitive trace metal and biological indicators of well-oxygenated conditions during Interval 1, including iron speciation (Tessin et al., 2016), micropaleontology (Lowery et al., 2017) and trace fossils (Savrda, 1998), it appears that the Pr/Ph ratios were not primarily controlled by sediment oxygenation in the Portland core. Elevated Pr/Ph ratios have also been observed in the Cenomanian-Turonian aged interval of the Portland core, despite this section recording intervals of oxygen limitation (Pancost et al., 1998).

The lack of relationship between Pr/Ph and redox is consistent with other research, which has shown that Pr/Ph can be affected by other environmental factors, and that care

should be taken when applying Pr/Ph ratios as a redox proxy (e.g. Ten Haven et al., 1987; Peters et al., 2005). Other sources of pristane and phytane in sediments have been suggested, including dihydrophytol a building block of kerogen and a component of archael cell membranes (Chappe et al., 1982). Tocopherols, a constituent of plant and algal lipid membranes, have also been proposed as a major source of pristane (Goosens et al., 1984).

Ratios of pristane and phytane to their corresponding n-alkane (Pr/n-$C_{17}$ and Ph/n-$C_{18}$) range between 0.52−2.04 and 0.29−0.94, respectively (Figure 8). Both ratios generally increase up-core, with the exception of elevated Ph/n-$C_{18}$ rations between 74.1 and 70.2 m (Figure 8). These results highlight that abundances of pristine and phytane relative to n-alkanes increase up-core. We propose that enhanced abundances of pristane and phytane in the Portland core are associated with an increase in the delivery of phototrophic organic matter - due to enhanced primary productivity.

## 5.0 Conclusions

Thermal maturity indices from the USGS Portland #1 core indicate that samples are somewhat immature with respect to oil formation. Sterane 20S/(20S+20R) results that fall significantly below the equilibrium value of 0.55 support thermal immaturity. However, $C_{30}$ hopane/moretane ratios and $C_{31}$ hopane 22S/(22S+22R) ratios are closer to equilibrium values. These results broadly agree with thermal maturity estimates from vitrinite reflectance and maximum temperatures, which suggest that the samples were nearing early oil formation.

Organic matter in the Portland core is dominated by marine algal and bacterial sources. The distribution of n-alkanes in the Portland record is characterized by abundant mid-chain length n-alkanes, especially n-$C_{21}$ and n-$C_{22}$ that may represent contributions from bacteria, fungi, yeast, and/or macrophytes. Because the WIS at this time was thought to be a relatively normal marine to brackish environment, this observation represents an expansion of

the depositional environments in which even-over-odd predominance has been observed in mid-chain length n-alkanes within the sedimentary record. The presence of long-chain n-alkanes (>$C_{25}$) with a clear odd-over-even predominance supports a small, but consistent, contribution of terrigenous organic matter.

Coincident with the high organic matter accumulation at the onset of Interval 2, there is an increase in the abundance of short-chain n-alkanes, suggesting an elevated contribution from algal organic matter. A significant increase in the contribution of algal organic matter during and after OAE 3 (Intervals 2 and 3) is supported by elevated relative abundances of $C_{28}$ and $C_{30}$ steranes. The observation of increased algal organic matter is coupled with the onset of enhanced organic carbon burial, as evidenced by the relationship between biomarker proxies and TOC. We suggest this enhancement of organic carbon burial was caused by an increase in algal primary productivity, as well as enhanced preservation of labile organic matter. Based on comparisons with paleo-redox reconstructions, the Pr/Ph ratios do not appear to be controlled by either redox changes. Conversely, pristane and phytane abundances are likely controlled by changing contributions of different algal sources associated with the higher marine algal input during Intervals 2 and 3.

## 6.0 Acknowledgements

We would like to thank the USGS Core Research Center for sample collection. This work was supported by ACS-PRF grant (#53845-ND8) to NDS and IH and a Scott Turner Award from the Department of Earth and Environmental Sciences at UM. AT was supported by an NSF-GRF (DGE 1256260). We are grateful to Phil Meyers for thoughtful discussions and manuscript comments.

## 7.0 References


Bourbonniere, R.A., Meyers, P.A. (1996), Sedimentary geolipid records of historical changes in the watersheds and productivities of Lakes Ontario and Erie, Limnology and Oceanography 41(2): 352-359.

Bray, E.E., E. D. Evans (1961), Distribution of n-paraffins as a chlue to recognition of source beds, Geochimica et Cosmochimica Acta 22, 2-15.

Brooks, J. D., K., Gould, J. W. Smith (1969), Isoprenoid hydrocarbons in coal and petroleum, Nature 222, 257-259.

Chappaz, A., T. Lyons, D. Gregory, C. Reinhard, B. Gill, C. Li, R. Large (2014), Does pyrite act as an important host for molybdenum in modern and ancient sediments?, Geochimica et Comsmochimica Acta, 126, 112-122.

Chaler, R., Dorronsoro, C., Grimalt, J.O., Agirrezabala, Fernandez-Mendiola, P.A., Garcia-Mondejar, J., Gomez-Perez, I., Lopez-Horgue, M. (2005), Distributions of C22–C30 even-carbon-number n-alkanes in Ocean Anoxic Event 1 samples from the Basque-Cantabrian Basin, Naturwissenschaften, 92(5), 221-225.

Chappe, B., P. Albrecht, W. Michaelis (1982), Polar lipids of archaebacteria in sediments and petroleums, Science 217, 65-66.

Collister, J., R. E. Summons, E. Lichtfouse, J. M. Hayes (1992), An isotopic biogeochemical study of the Green River oil shale, Organic Geochemistry 19, 265-276.

Dean, W. E.,M. A. Arthur (1998), Geochemical expressions of cyclicity in Cretaceous pelagic limestone sequences: Niobrara Formation, Western Interior Seaway, in Stratigraphy and Paleoenvironments of the Cretaceous Western Interior Seaway, edited by W. E. Dean and M. A. Arthur, pp. 227-255, SEPM Concepts in Sedimentology and Paleontology.

Didyk, B. M., B. R. T. Simoneit, S. C. Bassell, G. Eglinton (1978), Organic geochemical indicators of paleoenvironmental conditions of sedimentation, Nature 272, 216-222.

Eglinton, G., R. J. Hamilton (1967), Leaf Epicuticular Waxes, Science 156, 1322-1335.

Erickson BE, Helz GR (2000), Molybdenum (VI) speciation in sulfidic waters: Stability and lability of thiomolybdates, Geochimica et Cosmochimica Acta, 64, 1149-1158

Ficken, K.J., Li, B., Swain, D.L., Eglinton, G. (2000), An n-alkane proxy for the sedimentary input of submerged/floating freshwater aquatic macrophytes, Organic Geochemistry 31, 745–749.

Goosens, H., J. W. de Leeuw, P. A. Schenck, S. C. Brassell (1984), Tocopherols as likely precursors as likely precursors of pristane in ancient sediments and crude oils, Nature 312, 440-442.

Grimalt J., Albaiges J. (1987), Sources and occurrence of C12-C22 n-alkane distributions with even carbon- number preference in sedimentary environments, Geochimica et Cosmochimica Acta 51, 1379-1384.

Hedberg, H.D. (1968), Significance of high-wax oils with respect to genesis of petroleum, American Association of Petroleum Geologists Bulletin 52, 736–750.

Huang, W.-Y., W. G. Meninshein (1979), Sterols as ecological indicators, Geochimica et Cosmochimica Acta 43, 739-745.

Locklair, R.E., 2007, Causes and Consequences of Marine Carbon Burial: Examples from the Cretaceous Niobrara Formation and the Permian Brushy Canyon Formation, unpublished Ph.D. thesis, Northwestern University, 515 p.

Locklair, R., B. Sageman, A. Lerman (2011), Marine carbon burial flux and the carbon isotope record of Late Cretaceous (Coniacian-Santonian) Oceanic Anoxic Event III, Sedimentary Geology, 235(1-2), 38-49.

Lowery, C. M., R. M. Leckie, B. B. Sageman (2017), Micropaleontological evidence for redox changes in the OAE3 interval of the US Western Interior: Global vs. local processes, Cretaceous Research 69 (34-48).

Mackenzie, A. S., R. K. Patience, J. R. Vandenbroucke, B. Durand (1980), Molecular parameters of maturation in the Toarcian shales, Paris Basin, France—I. Changes in the configuration of acyclic isoprenoid alkanes, steranes, and triterpanes, Geochimica et Cosmochimica Acta 44, 1709-1721.

Meyers, P. A. (1997), Organic geochemical proxies of paleoceanographic, paleolimnologic, and paleoclimatic processes, Organic Geochemistry 27, 213-250.

Meyers, S. R., B. B. Sageman, T. W. Lyons (2005), Organic carbon burial rate and the molybdenum proxy: Theoretical framework and application to Cenomanian-Turonian oceanic anoxic event 2, Paleoceanography, 20(2).

Moldowan, J. M., W. K. Seifert, E. J. Gallegos (1985), Relationship between petroleum composition and depositional environment of petroleum source rocks, American Association of Petroleum Geologists Bulletin 69, 1255-1268.

Moldowan, J. M., F. J. Fago, C. Y. Lee (1990), Sedimentary 24-n-propylcholestanes, molecular fossils diagnostic of marine algae, Science 247, 309-312.

Nishimura M., Baker E. W. (1986), Possible origin of n-alkanes with a remarkable even-to-odd predominance in recent marine sediments, Geochimica et Cosmochimica Acta 50, 299-305.

Ogihara S, Ishiwatari R (1998) Unusual distribution of hydrocarbons in a hydrothermally altered phosphorite nodule from Kusu Basin, northern Kyushu, Japan. Org Geochem 29:155–161.

Pancost, R.D., Freeman, K.H., and Arthur, M.A. (1998), The Organic Geochemistry of the Cretaceous Western Interior Seaway: A Trans-Basinal Evaluation. In: Dean, W.E., and Arthur, M.A. (Eds) SEPM Concepts in Sedimentology and Paleontology No. 6

Peters, K.E., Walters, C. C., Moldowan, J.M. (2005), The Biomarker Guide: Volume 2 Biomarkers and Isotopes in Petroleum Exploration and Earth History, Prentice Hall, Englewood Cliffs, NJ.

Powell, T. G., D. M. McKirdy (1973), Relationship between ratio of pristane to phytane, crude oil composition and geological environments in Australia, Nature 243, 37-39.

Pratt, L. M., M. A. Arthur, W. E. Dean, P. A. Scholle (1993), Paleo-oceanographic Cycles and Events during the Late Cretaceous in the Western Interior Seaway of North America, in Evolution of the Western Interior Basin, edited by W. G. E. Caldwell and E. G. Kauffman, pp. 333-354, GAC Special Paper.

Sageman, B., M. Arthur (1994), Early Turonian paleogeographic/paleobathymetric map, Western Interior, US in Caputo, M. V., Peterson J. A., and Franczyk, K.J., eds., Mesozoic Systems of the Rocky Mountain Region, USA: SEPM, Rocky Mountain Section, 457- 470.

Savdra, C. E. (1998), Ichnocoenoses of the Niobrara Formation: Implications for benthic oxygenation histories, in Stratigraphy and Paleoenvironments of the Cretaceous Western Interior Seaway, edited by W. E. Dean and M. A. Arthur, pp. 227–255, SEPM Concepts in Sedimentology and Paleontology, Tulsa, Okla.

Scanlan, R. S., J. E. Smith (1970) An improved measure of the odd-to-even predominance in the normal alkanes of sediment extracts and petroleum, Geochimica et Cosmochimica Acta 34, 611-620.

Schenk, P. A. (1968) The predominance of the C22 n-alkane in rock extracts, in: Advances inorganic geochemistry, eds. P. A. Schenk and I. Havenaar, 261-268, Pergamon Press.

Scott, G. R., W. A. Cobban (1964), Stratigraphy of the Niobrara Formation at Pueblo, Colorado, U.S. Geological Survey Professional Paper, 454-L, L1–L30.

Seifert, W. K., J. M. Moldowan (1986), Use of biological markers in petroleum exploration, In: Methods in Geochemistry and Geophysics, Vol 24, R. B. Johns, eds., Elsevier, Amsterdam, 261-290.

Sonnenberg, S.A. (2011), The Niobrara Petroleum System: A New Resource Play in the Rocky Mountain Region, in Estes-Jackson, J.E., Anderson, D.S., ed., Revisiting and Revitalizing the Niobrara in the Central Rockies: Denver, CO, Rocky Mountain Association of Geologists, p. 13-32.

Ten Haven, H. L., J. W. de Leeuw, J. Rullkotter, J. A. Sinninghe Damste (1987), Restricted utility of the pristane/phytane ratio as a paleoenvironmental indicator, Nature 330, 641-643.

Tessin, A., I. Hendy, N. Sheldon, B. Sageman (2015), Redox-controlled preservation of organic matter during "OAE 3" within the Western Interior Seaway, Paleoceanography 30 (6), 702-717.

Tessin, A., N. Sheldon, I. Hendy, A. Chappaz (2016), Iron limitation in the Western Interior Seaway during the Late Cretaceous OAE 3 and its role in phosphorus recycling and enhancing organic matter preservation, Earth and Planetary Science Letters 449, 135-144.

Tissot, B. (1979), Effects on prolific petroleum source rocks and major coal deposits caused by sea-level changes Nature 277, p. 463-465.

Viso, A. C., Marty, J. C. (1993), Fatty acids from 28 marine microalgae, Phytochemistry 34, 1521–1533.

Volkman, J.K., Farrington, J.W. Gagosian, R.B. (1987), Marine and terrigenous lipids in coastal sediments from the Peru upwelling region at 15ºS: Sterols and triterpene alcohols, Organic Geochemistry 11, 463-477.

Volkman, J.K. (2003), Sterols in microorganisms, Applied Microbiology and Biotechnology 60, 495-506.

Wagreich, M. (2012), "OAE 3"-regional Atlantic organic carbon burial during the Coniacian-Santonian, Climate of the Past 8, 1447–1455.

Welte DH, Waples DW (1973), Uber die Bevorzugung geradzahlinger n-alkane in sedimentgesteinen, Naturwissenschaften 60:516–517.

**Figure Captions**

Figure 1. (a) Map of the Coniacian lithology of the Western Interior Seaway with Turonian paleobathymetry (adapted from Sageman and Arthur (1995). Darker colors represent relatively deeper water depths. (b) stratigraphy and total organic carbon (TOC) from the USGS Portland #1 core (adapted from Tessin et al., 2015). Intervals 1, 2, and 3 are designated with dashed lines. Interval 1 includes the basal Fort Hays Limestone and the lower shale limestone (lsl) subunit of the Smoky Hill Chalk. Interval 2 includes the lower shale (ls) and lower limestone (ll) subunits of the Smoky Hill Chalk. Interval 3 includes the middle shale (ms) subunit of the Smoky Hill Chalk. Black lines represent major rivers draining into the WIS.

Figure 2. Characteristic (a and b) m/z 191 and (c and d) 217 chromatograms from (bottom) the lower (62.84 m) and (top) upper (30.38) portions of the core. Hopanes and steranes are.

Figure 3. Thermal maturity indicators from the USGS Portland #1 core, (a) $C_{27}$ and $C_{29}$ 5α,14α,17α(H)-sterane 20S/(20S+20R), (b) $C_{30}$ Moretane/Hopane ratios and $C_{31}$ 17α-hopane 22S/(22S+22R), (c) vitrinite reflectance and (d) Rock Eval derived maximum temperatures from Locklair (2007) with expected maturity values. Dashed lines in (a) and (b) indicate equilibrium values for biomarker thermal maturity indices (Seifert and Moldowan, 1986).

Figure 4. Characteristic m/z 57 chromatograms from (a) the lower (62.84 m) and (b) upper (30.38) portions of the core. Most abundant n-alkanes and isoprenoids are labeled.

Figure 5. Relative abundances of odd (dark blue) and even (light blue) chain length n-alkanes and isoprenoids (red; N–norpristane; Pr–pristane; Ph–phytane) within each sample. Brackets indicate short-, mid-, and long-chain length n-alkanes. Stratigraphic interval is indicated at the top of each column. Total organic carbon concentrations for each sample are included in gray.

Figure 6. (a) Terrestrial-aquatic ratios, (b) sterane $C_{27}$/ ($C_{27}$–$C_{30}$) ratios, (c) sterane $C_{28}$/ ($C_{27}$–$C_{30}$)ratios, (d) $C_{29}$/ ($C_{27}$–$C_{30}$), (e) $C_{30}$/ ($C_{27}$–$C_{30}$), and (f) sterane/hopane ratios from the USGS Portland #1 core. Gray symbols indicate samples with >1% TOC and white symbols indicate samples with <1% TOC. Dashed lines indicate Intervals 1, 2, and 3 as designated by Tessin et al. (2015).

Figure 7. Ternary diagram of steranes $C_{27}$ R, $C_{28}$ R, and $C_{29}$ R from the USGS Portland #1 core. Gray symbols indicate samples with >1% TOC and white symbols indicate samples with <1% TOC.

Figure 8. Pristane/phytane, pristane/ n-$C_{17}$, and phytane/ n-$C_{18}$ from the USGS Portland #1 core. White, gray, and black symbols indicate samples with Mo concentrations of <1 ppm, 1–20 ppm, and >20 ppm, respectively. Dashed lines indicate Intervals 1, 2, and 3 as designated by Tessin et al. (2015).

**Figure 1**

Figure 1.

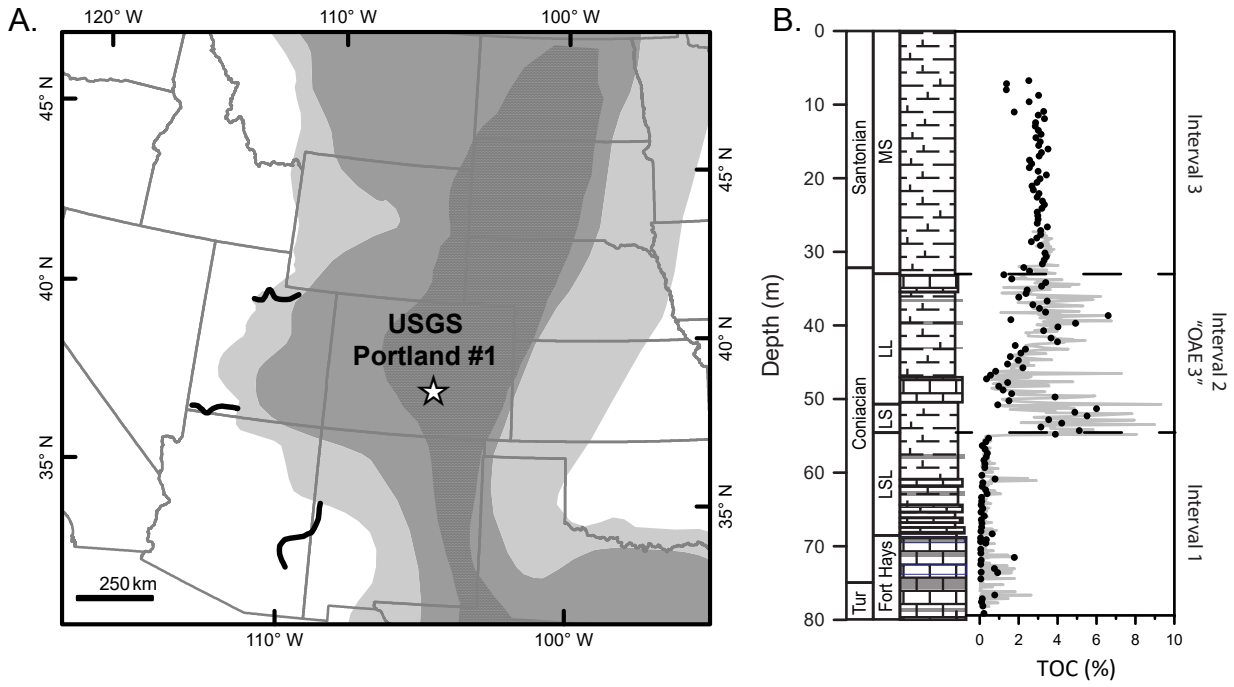

**Figure 2**

Figure 2.

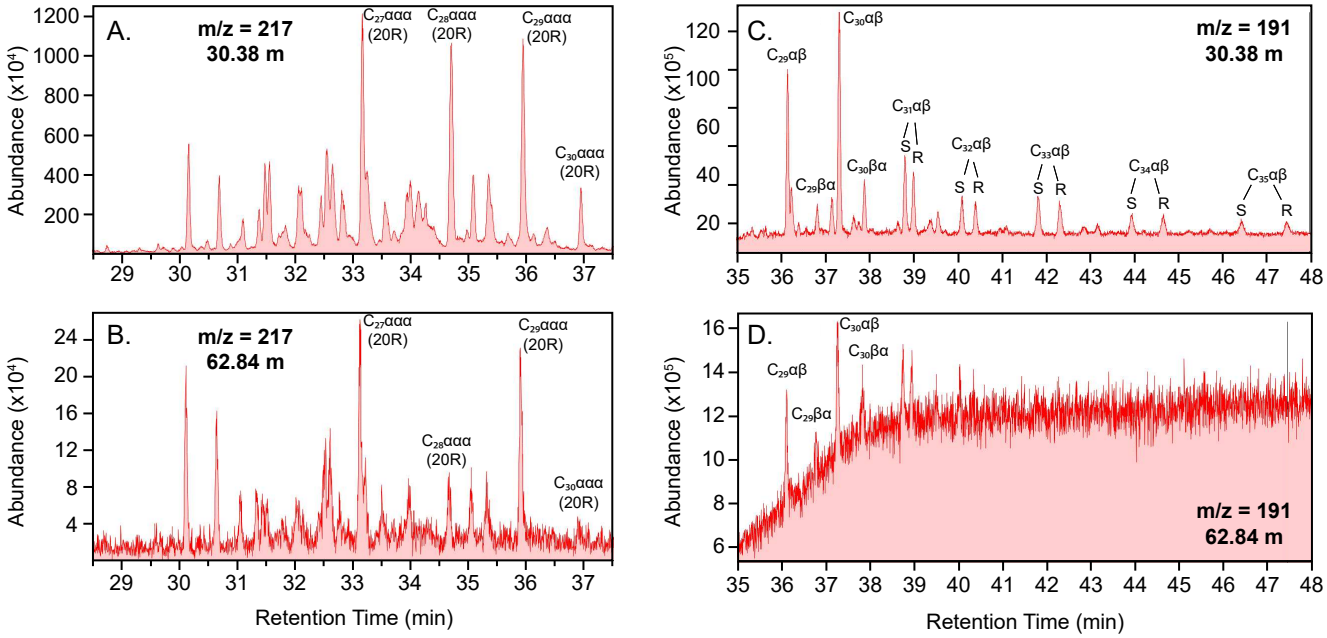

**Figure 3**

Figure 3.

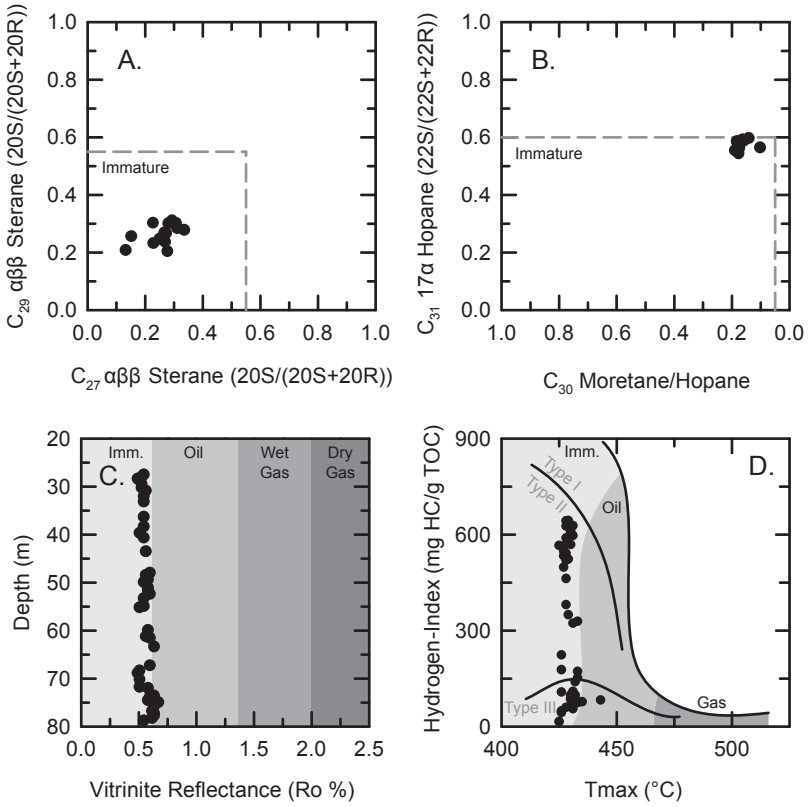

**Figure 4**

Figure 4.

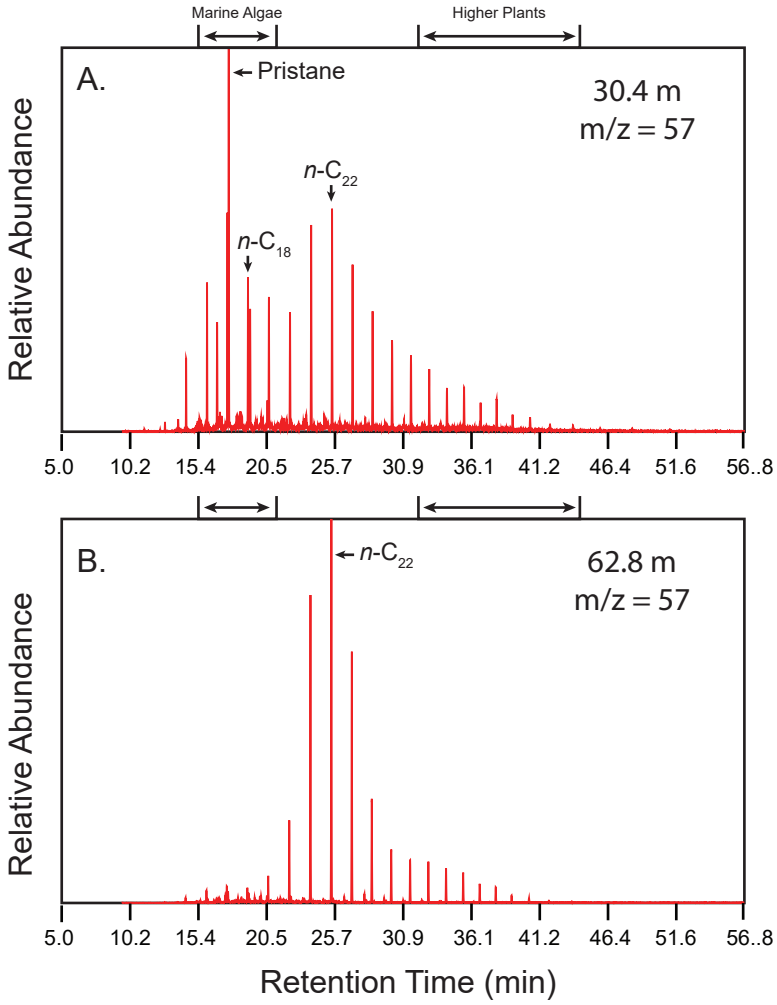

**Figure 5**

Figure 5.

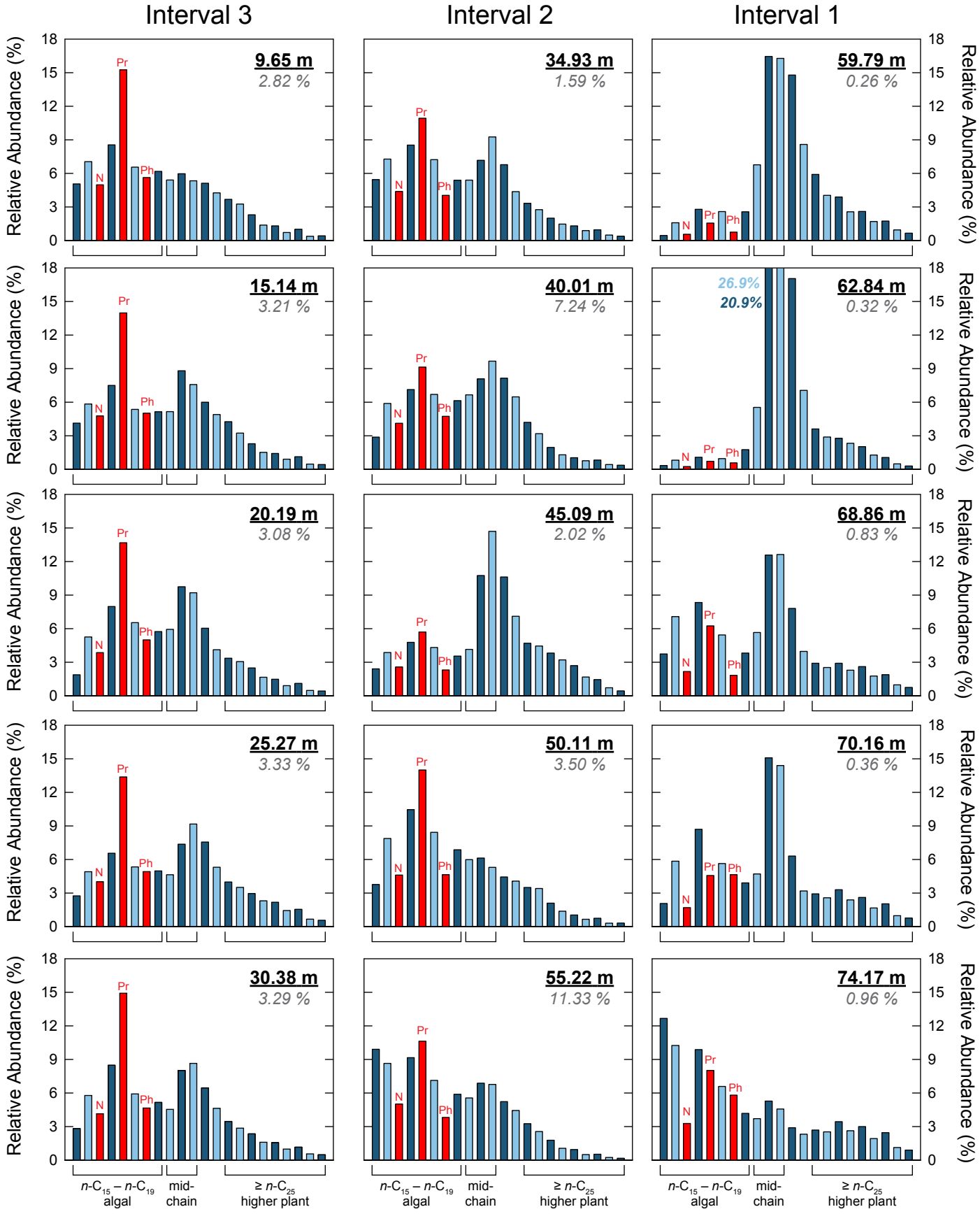

**Figure 6**

Figure 6.

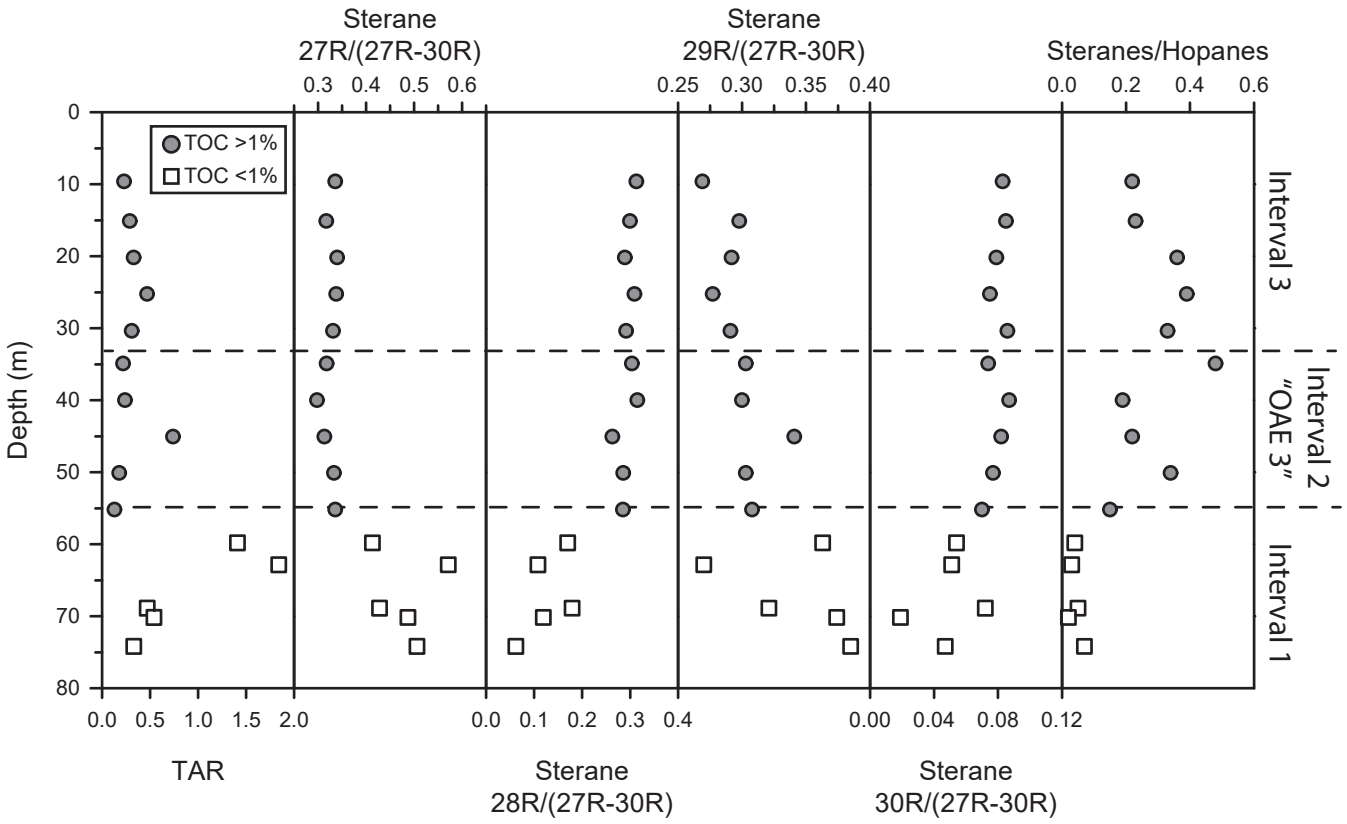

**Figure 7**

Figure 7.

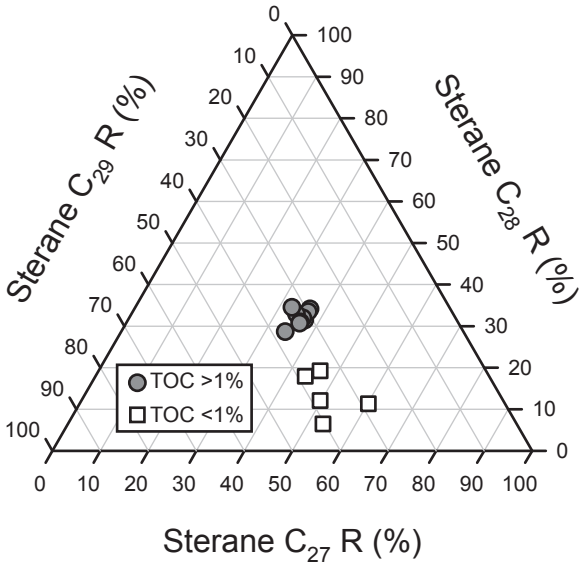

**Figure 8**

Figure 8.

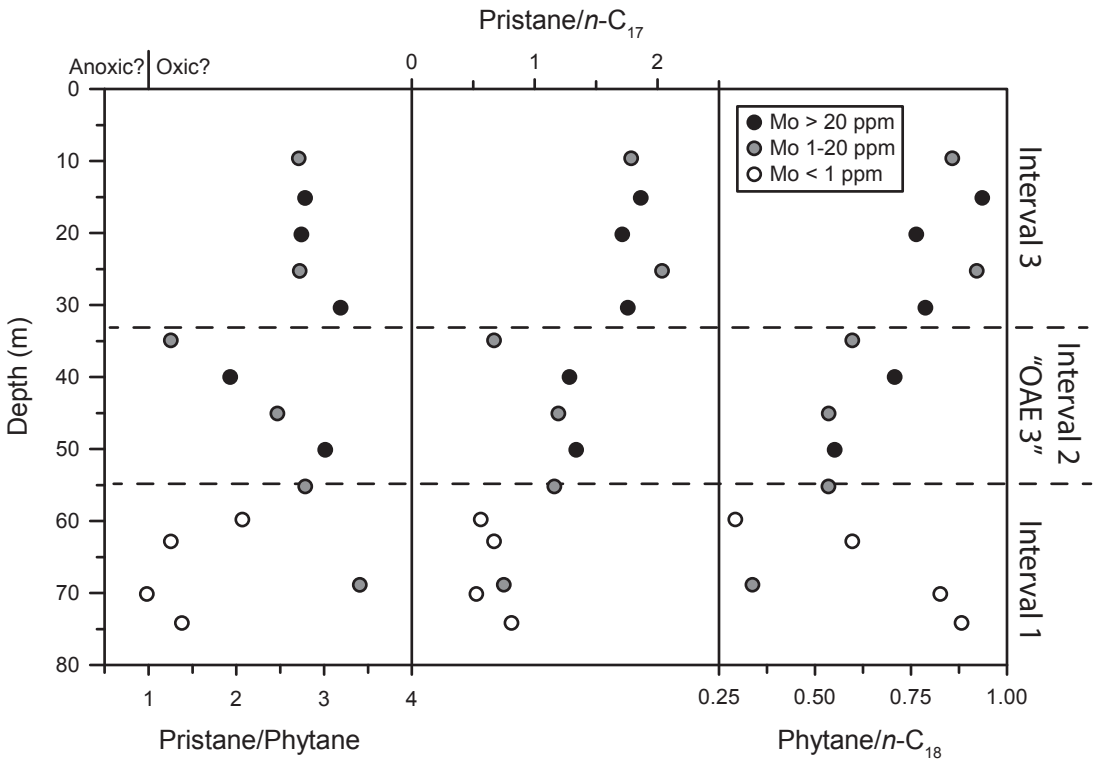

**Table 1**

Table 1
Thermal maturity biomarker results for the USGS Portland #1 core

| Depth (m) | $C_{27}$ αββ sterane 20S/(20S+20R) | $C_{29}$ αββ sterane 20S/(20S+20R) | $C_{30}$ moretane/ hopane | $C_{31}$ Hopane 20S/(20S+20R) | $C_{32}$ Hopane 20S/(20S+20R) |
|---|---|---|---|---|---|
| | **<0.55** | **<0.55** | **>0.05** | **<0.6** | **<0.6** |
| 9.65 | 0.266 | 0.269 | 0.162 | 0.593 | 0.621 |
| 15.14 | 0.269 | 0.237 | 0.194 | | |
| 20.19 | 0.229 | 0.233 | 0.175 | 0.561 | 0.518 |
| 25.27 | 0.261 | 0.256 | 0.182 | 0.586 | 0.522 |
| 30.38 | 0.249 | 0.247 | 0.189 | 0.555 | 0.498 |
| 34.93 | 0.280 | 0.301 | 0.174 | 0.565 | 0.537 |
| 40.01 | 0.293 | 0.311 | 0.180 | 0.559 | 0.665 |
| 45.09 | 0.311 | 0.284 | 0.102 | 0.565 | 0.595 |
| 50.11 | 0.307 | 0.302 | 0.157 | 0.588 | 0.610 |
| 55.22 | 0.273 | 0.267 | 0.182 | 0.583 | 0.550 |
| 59.79 | 0.152 | 0.257 | | | |
| 62.84 | 0.277 | 0.205 | | | |
| 68.86 | 0.227 | 0.303 | 0.176 | 0.544 | 0.778 |
| 70.16 | 0.336 | 0.278 | | | |
| 74.17 | 0.132 | 0.208 | 0.141 | 0.597 | 0.296 |

**Table 2**

Table 2. Organic matter source biomarker results for the USGS Portland #1 core

| Depth (m) | Carbon Preference Index (CPI) | Odd-Even Preference ($OEP_{31}$) | Odd-Even Preference ($OEP_{23}$) | Terrestrial to Aquatic Ration (TAR) | Sterane 27R/ (27R-30R) | Sterane 28R/ (27R-30R) | Sterane 29R/ (27R-30R) | Sterane 30R/ (27R-30R) | Steranes/ Hopanes | Pr/Ph | Pr/n-$C_{17}$ | Ph/n-$C_{18}$ |
|---|---|---|---|---|---|---|---|---|---|---|---|---|
| 9.65 | 1.04 | 1.75 | 1.05 | 0.23 | 0.336 | 0.313 | 0.269 | 0.083 | 0.22 | 2.710 | 1.785 | 0.858 |
| 15.14 | 1.00 | 1.56 | 0.98 | 0.29 | 0.317 | 0.300 | 0.298 | 0.085 | 0.23 | 2.782 | 1.863 | 0.936 |
| 20.19 | 0.96 | 1.55 | 0.93 | 0.33 | 0.340 | 0.289 | 0.292 | 0.079 | 0.36 | 2.741 | 1.714 | 0.764 |
| 25.27 | 1.02 | 1.43 | 0.98 | 0.47 | 0.338 | 0.309 | 0.277 | 0.075 | 0.39 | 2.721 | 2.037 | 0.921 |
| 30.38 | 1.00 | 1.43 | 0.95 | 0.31 | 0.331 | 0.292 | 0.291 | 0.086 | 0.33 | 3.187 | 1.758 | 0.788 |
| 34.93 | 0.98 | 1.36 | 0.96 | 0.22 | 0.318 | 0.304 | 0.303 | 0.074 | 0.48 | 2.701 | 1.282 | 0.559 |
| 40.01 | 0.95 | 1.32 | 0.95 | 0.24 | 0.298 | 0.315 | 0.300 | 0.087 | 0.19 | 1.929 | 1.284 | 0.708 |
| 45.09 | 0.95 | 1.24 | 0.91 | 0.74 | 0.313 | 0.263 | 0.341 | 0.082 | 0.22 | 2.468 | 1.192 | 0.536 |
| 50.11 | 0.94 | 1.53 | 0.97 | 0.18 | 0.333 | 0.286 | 0.303 | 0.077 | 0.34 | 3.012 | 1.339 | 0.551 |
| 55.22 | 0.96 | 1.44 | 0.93 | 0.13 | 0.336 | 0.285 | 0.308 | 0.070 | 0.15 | 2.784 | 1.160 | 0.535 |
| 59.79 | 1.12 | 1.29 | 1.12 | 1.41 | 0.413 | 0.170 | 0.363 | 0.054 | 0.04 | 2.067 | 0.560 | 0.293 |
| 62.84 | 0.98 | 1.22 | 0.96 | 1.84 | 0.571 | 0.108 | 0.270 | 0.051 | 0.03 | 1.253 | 0.668 | 0.597 |
| 68.86 | 1.02 | 1.33 | 0.94 | 0.47 | 0.428 | 0.179 | 0.321 | 0.072 | 0.05 | 3.406 | 0.748 | 0.337 |
| 70.16 | 0.94 | 1.47 | 0.79 | 0.54 | 0.487 | 0.119 | 0.374 | 0.019 | 0.02 | 0.980 | 0.525 | 0.826 |
| 74.17 | 1.12 | 1.53 | 0.92 | 0.33 | 0.506 | 0.062 | 0.385 | 0.047 | 0.07 | 1.379 | 0.811 | 0.882 |

**Supplemental Table 1**

**Click here to download Supplementary Material (for online publication only): Supplemental Table 1-2.docx**

**Supplemental Table 2**

**Click here to download Supplementary Material (for online publication only): Supplemental Table 2-2.docx**